JOURNAL OF GEOPHYSICAL RESEARCH, VOL. 91, NO. C12, PAGES 14,192–14,206, DECEMBER 15, 1986

A Model of the Seasonal Cycle in the Tropical Atlantic Ocean

S. G. H. PHILANDER AND R. C. PACANOWSKI

Geophysical Fluid Dynamics Laboratory, NOAA, Princeton University, Princeton, New Jersey

In the western tropical Atlantic, seasonal variations in the surface winds and in the ocean are dominated by an annual harmonic. A simulation with a general circulation model indicates that the response in the western side of the basin is an equilibrium one practically in phase with the local winds. It includes the following: large vertical excursions of the thermocline that have a 180° change in phase across 8°N approximately; a change in the direction of the North Brazilian Coastal Current, which flows continuously along the coast between December and May but which veers offshore near 5°N to feed the North Equatorial Countercurrent during the other months; and a seasonal reversal of the countercurrent. To the east of 30°W, seasonal changes in the model have a prominent semiannual harmonic in phase with the local winds but only partially attributable to forcing at that frequency. The transients excited by the abrupt intensification of the southeast tradewinds in May happen to have a phase essentially the same as that of the semiannual forcing. These transients decay by the end of the calendar year, so that the seasonal cycle that starts with the intensification of the winds in May can be treated as an initial value problem as far as the upper ocean, above the thermocline, is concerned. The winds along the equator determine the response of the surface equatorial layer in the Gulf of Guinea but play a minor role in the seasonal upwelling along the coast near 5°N. That upwelling is strongly influenced by changes in both components of the wind, and in the curl of the wind, over the Gulf of Guinea.

1. INTRODUCTION

The response of the Tropical Atlantic Ocean to the seasonally varying surface winds includes a number of striking phenomena: the separation of the intense Brazilian Coastal Current from the coast during certain months of the year [*Bruce et al.*, 1984]; the seasonal reversal of the North Equatorial Countercurrent in the western side of the ocean basin [*Garzoli and Katz*, 1983; *Merle*, 1983; *Merle and Arnault*, 1985; *Richardson and McKee*, 1984]; the penetration of the Equatorial Undercurrent into the Gulf of Guinea, where the prevailing eastward winds usually maintain pressure gradients that oppose the undercurrent [*Hisard*, 1973; *Hisard and Morlière*, 1973; *Voituriez*, 1983]; and seasonal upwelling along the northern and eastern coasts of the Gulf of Guinea where the local winds do not vary seasonally [*Houghton*, 1976; *Picaut*, 1983]. There have been several studies of the response of the Atlantic to idealized winds but thus far only two attempts to calculate the response of the tropical Atlantic to realistic winds. *Busalacchi and Picaut* [1983] use a linear shallow water model, and *du Penhoat and Triguier* [1985] use a continuously stratified linear model. These calculations succeed in reproducing some of the observed seasonal changes, in the dynamic topography, for example, with reasonable accuracy. The models are poor near the equator, where nonlinear effects are important.

This paper describes results from a multilevel, primitive equation numerical model of the tropical Atlantic Ocean which is forced with climatological monthly mean winds. A comparison of the available measurements with results from the model indicates that the simulation is realistic. (For a preliminary quantitative comparison between data from the model and oceanic measurements see *Katz* [1984], *Garzoli and Philander* [1985], and *Richardson and Philander* [1986]. Further studies along these lines are in progress.) The picture of the seasonal cycle as obtained from the model is far more complete than that which can be obtained from the available scattered measurements of a few variables. Not only does the model resolve all relevant spatial and temporal scales, but it also describes variables that are difficult to measure, the vertical component of the velocity, for example.

A realistic model of the oceanic circulation is a powerful tool with which to address questions concerning the dynamics of this circulation. A question of considerable interest concerns the relative merits of the two views that can be taken of the seasonal variations in the tropical Atlantic. One view emphasizes the cyclic aspect of these variations and has motivated studies of the oceanic response to sinusoidally varying winds with a period of 1 year [*Cane and Sarachik*, 1981; *Philander and Pacanowski*, 1981; *McCreary et al.*, 1984]. The other view emphasizes the nonsinusoidal aspect of the wind variations, specifically the abrupt intensification of the southeast trades in May and June when the intertropical convergence zone (ITCZ) starts to move away from the equator. This latter set of studies [*Moore et al.*, 1978; *Katz and Garzoli*, 1982; *Weisberg and Tang*, 1983] treats the oceanic response to the intensification of the trades in May and June each year as an initial value problem by assuming that the ocean, by that time, has lost all memory of earlier changes in the winds. The validity of this assumption has not been established, but these studies do explain some of the features of the observed seasonal cycle, and they provide a simpler picture of the seasonal changes than that available from studies of the response to periodic winds. The response to periodic winds is in general complex because all the waves, and their reflections, that are available at the forcing frequency are superimposed on the directly wind-driven motion. In this paper the realistic general circulation model is used to determine the extent to which the initial value approach is relevant to the seasonal cycle of the tropical Atlantic Ocean.

Paper number 6C0450.

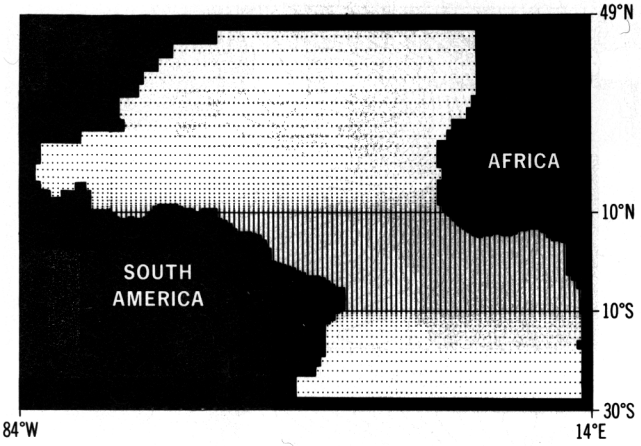

Fig. 1. Distribution of grid points in the model.

This paper is organized as follows: Section 2 describes the model, and section 3 gives an overview of the results. The subsequent sections focus on the three main regions, namely, the equatorial zone, the western side of the basin, and the Gulf of Guinea. Companion papers compare results from linear and nonlinear versions of the model, discuss the properties of waves excited by the unstable surface currents, and describe the mass and heat budgets of the simulation in more detail [*Philander and Pacanowski*, 1986, this issue; *Philander et al.*, this issue]. These studies by no means exhaust the analysis of data from the model, which is continuing.

2. The Model

The Atlantic Ocean model extends from 28°S to 50°N latitude. The coastlines and grid point distribution are shown in Figure 1. The longitudinal resolution is a constant 100 km, with a latitudinal resolution of 33 km between 10°S and 10°N increasing gradually poleward of this region. At 25°N the latitudinal spacing is 200 km. The topography of the ocean floor is taken into account, except that islands are 150 m below the sea surface and the coastal shelf is 50 m below the sea surface. There are 27 levels in the vertical; the upper 100 have a resolution of 10 m.

The primitive equations are solved numerically by means of finite differencing methods discussed by *Bryan* [1969]. The use of Richardson number dependent vertical mixing coefficients is explained in detail by *Pacanowski and Philander* [1981]. In the upper 10 m of the model the coefficient of vertical eddy viscosity has a minimum value of 10 $cm^2\ s^{-1}$ to compensate for mixing by the high-frequency wind fluctuations, which are absent from the monthly mean winds. In the deep ocean, where vertical mixing is negligible, vertical viscosity has the value of molecular viscosity. The coefficients of horizontal eddy viscosity and diffusivity are 2×10^7 $cm^2\ s^{-1}$ equatorward of 10° latitude; poleward of this they increase gradually to a value of 7×10^7 $cm^2\ s^{-1}$ at 50°N. Unstable temperature gradients are eliminated instantaneously by mixing heat vertically to a depth that ensures a stable density gradient.

Poleward of 20°S and 30°N the equation for temperature T gains a term $\gamma(T - T^*)$ where T^* is the prescribed monthly mean climatological temperature for the region under consideration, and γ is a Newtonian cooling coefficient. Its value is 1/(2 days) near the zonal boundaries and decreases to a value of zero equatorward of 30°N and 20°S. This device mitigates the effect of the artificial zonal walls along the southern and northern boundaries of the ocean and forces the solution toward the climatology in these regions.

The heat flux across the ocean surface is

$$Q = \mathrm{SW} - \mathrm{LW} - Q_S - Q_E$$

The solar short-wave heating SW is taken to be 500 Ly d^{-1} equatorward of 20° latitude and decreases linearly to 300 Ly d^{-1} between 20° and 45° latitude. The long-wave back radiation LW has the constant value of 115 Ly d^{-1}. The sensible heat flux is

$$Q_S = \rho C_D C_p V(T_0 - T_A)$$

and the evaporation is

$$Q_E = \rho C_D L V[e_s(T_0) - \gamma e_s(T_A)](0.622/p_A)$$

where the saturation vapor temperature is

$$e_s(T) = 10^{[9.4-(2353/T)]}$$

Here $\rho = 1.2 \times 10^{-3}$ g cm^{-3}, $L = 595$ cal g^{-1}, $C_D = 1.4 \times 10^{-3}$, $p = 1013$ mbar, $C_p = 0.24$ cal g^{-1} °C^{-1}, T_0 is the sea surface temperature in degrees Kelvin, T_A is the atmospheric temperature at the surface, and V is the surface wind speed; the relative humidity γ is assigned the constant value 0.8. No provision is made for clouds. The sensible heat flux is found to be of secondary importance, so that variations in heat flux are primarily a consequence of change in the evaporation. Since evaporation depends on wind speed, avoidance of excessively high temperatures in regions of weak winds requires that the wind speed be not less than 4.8 m s^{-1}. This minimum parameterizes evaporation caused by high-frequency wind fluctuations that are absent from the mean monthly winds. This restriction applies only to the evaporative term.

The initial conditions for the model are zero currents and the climatological temperature and salinity fields of January [*Levitus*, 1982]. Monthly averaged climatological winds

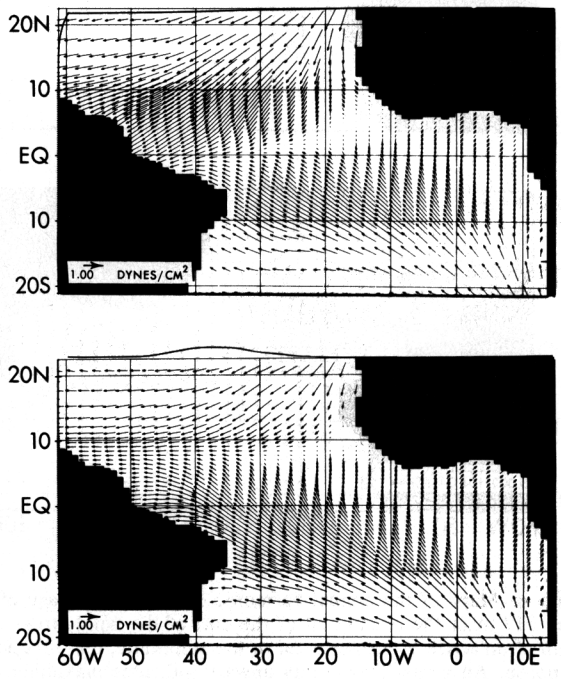

Fig. 2. Monthly mean wind stress vectors for April and October.

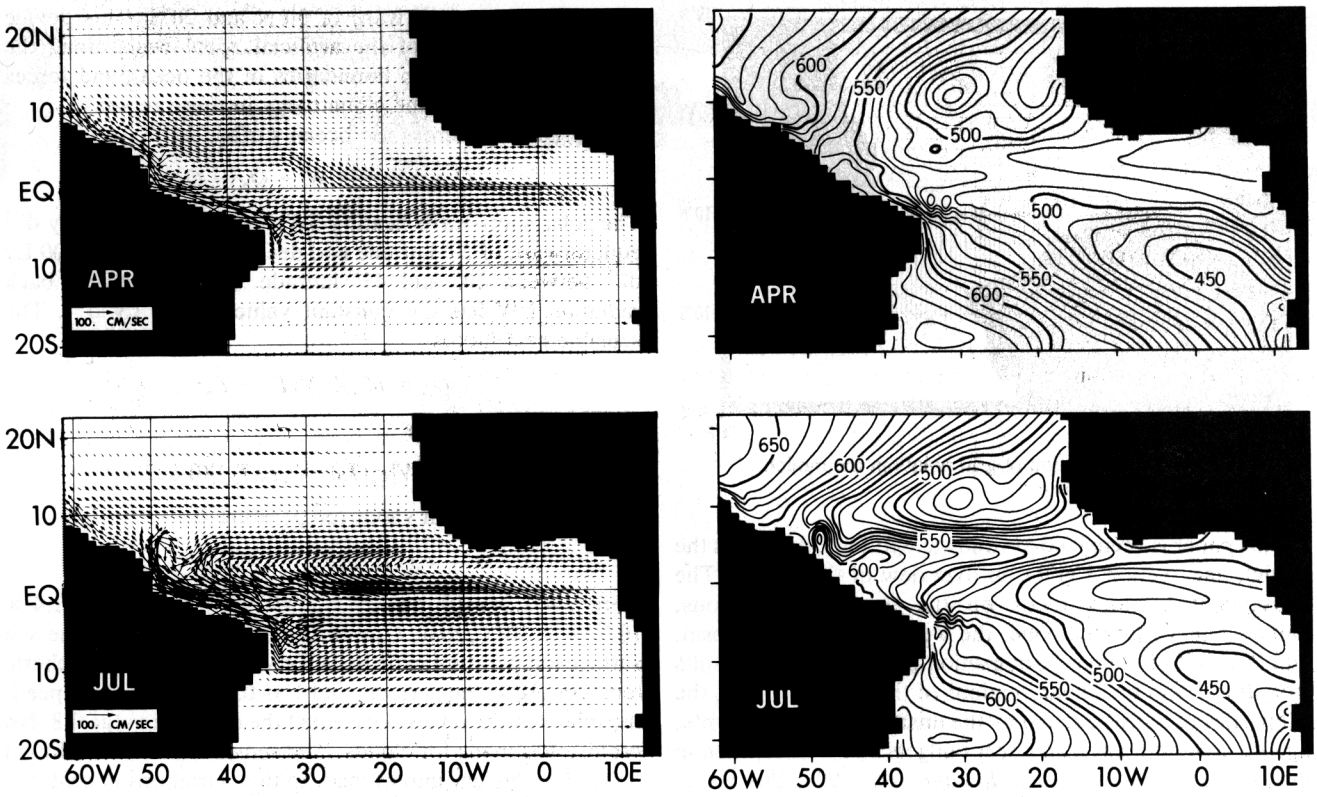

Fig. 3. Maps of surface current vectors and heat storage of the upper ocean (which is defined to be the vertical integral of the temperature from the surface to a depth of 317 m and has units of 10^3 cal cm^{-2}) for April 15 and July 15.

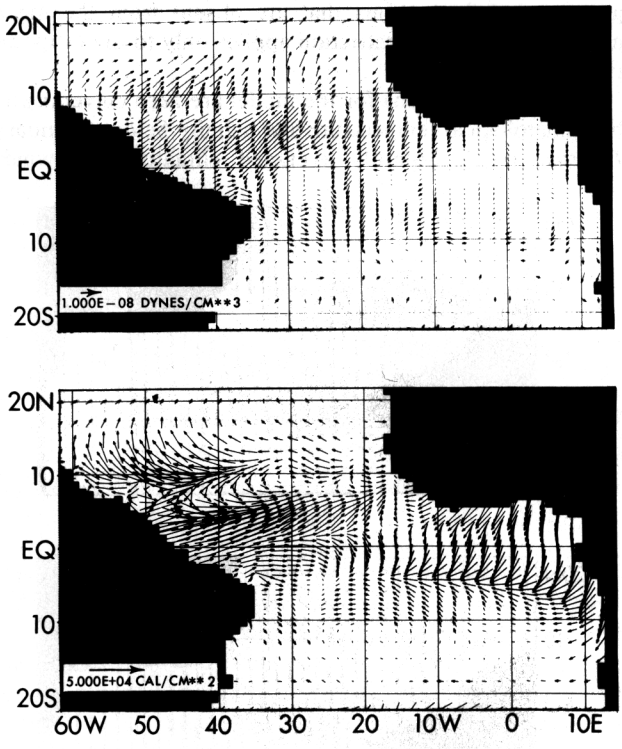

Fig. 4. Maps of the annual harmonic of the heat storage of the upper 317 m of the ocean and of the curl of the wind stress. The length of an arrow is proportional to the amplitude; the direction is the phase. An arrow that points upward indicates maximum heat storage on July 15. Phase increases in a clockwise direction.

[*Hellerman and Rosenstein*, 1983] then force the model for 2 years, by which time the model has an equilibrium seasonal cycle. The results to be shown here are from the third year of the simulation.

3. Overview of the Results

The southeast and northeast trade winds that prevail over the tropical Atlantic Ocean converge on the intertropical convergence zone, which moves meridionally with the seasons; it is furthest north in August and September when the southeast trades are most intense and is closest to the equator during March and April when the southeast trades are weak (Figure 2).

In April, when the intensity of winds near the equator is at a minimum, zonal density gradients within 10° latitude of the equator are small. The surface currents at that time are weak and generally westward except for the intense Brazilian Coastal Current, which flows continuously along the coast into the Gulf of Mexico (Figure 3). The northward movement of the ITCZ, and the associated intensification of the southeast trades, which starts in May, has a dramatic effect on the ocean. To the south of 3°N the westward surface flow intensifies considerably, and to the north of 3°N the westward surface flow is replaced by strong eastward North Equatorial Countercurrent. The latter current is fed by the Brazilian Coastal Current, which now separates from the coast near 5°N. The thermocline develops a deep trough near 3°N. This, together with the ridge of the thermocline near 10°N, reflects the geostrophic balance of the countercurrent. The westward surface flow to the south of 3°N drains warm surface waters from the Gulf of Guinea, where the

thermocline shoals, and transfers it to the western side of the basin, where the thermocline deepens. This deepening is most pronounced not at the equator, where upwelling is intense, but near 3°N, where there is downwelling. Northward motion in the surface layers and equatorward motion at the depth of the thermocline close the shallow meridional cell between 3°N and the equator. The intensity of this cell has very large spatial and temporal fluctuations associated with instabilities that result when the strengthening winds increase the shear between the westward surface flow to the south of 3°N and the eastward flow further north. The fluctuations are evident in Figures 6 and 12 which show that they appear from June onward in the western equatorial region. *Philander et al.* [this issue] describe their properties in more detail.

The intensification of the trade winds stops after mid-June in the region to the east of 30°W but continues into September to the west of 30°W (Figure 5). The winds in the east weaken somewhat in July and August but then intensify again in November so that the seasonal changes to the east of 30°W have a significant semiannual signal. To the west of 30°W, on the other hand, variations are dominated by the annual harmonic. The oceanic response to these seasonal changes in the winds is remarkable for being highly correlated, and in phase, with the local winds in both the western and eastern sides of the basin. In the western equatorial Atlantic the thermocline deepens while the local winds intensify (May to September) and shoals while the local winds relax. In the Gulf of Guinea, upwelling is at a maximum in June and again in December, when the westward winds to the west of the Greenwich meridian have maxima. From July into September the thermocline in the east deepens, while the local westward winds relax. Hence the thermocline is sinking all along the equator between July and September while the trades are intensifying in the west and relaxing in the east. Finally, during the early months of the year, when the winds everywhere along the equator become weak, the thermocline returns to an almost horizontal position. By this time the North Equatorial Countercurrent is absent from the surface layers in the west (it persists below the surface), and the Brazilian Coastal Current once again flows continuously along the coast into the Gulf of Mexico.

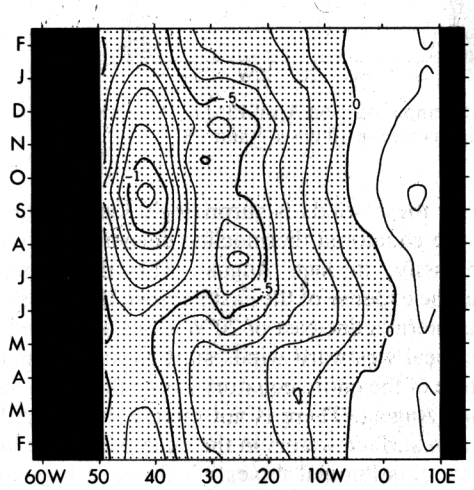

Fig. 5. Seasonal changes in the zonal component of the wind stress along the equator. The wind is westward in shaded regions. The contour interval is 0.1 dyn cm^{-2}.

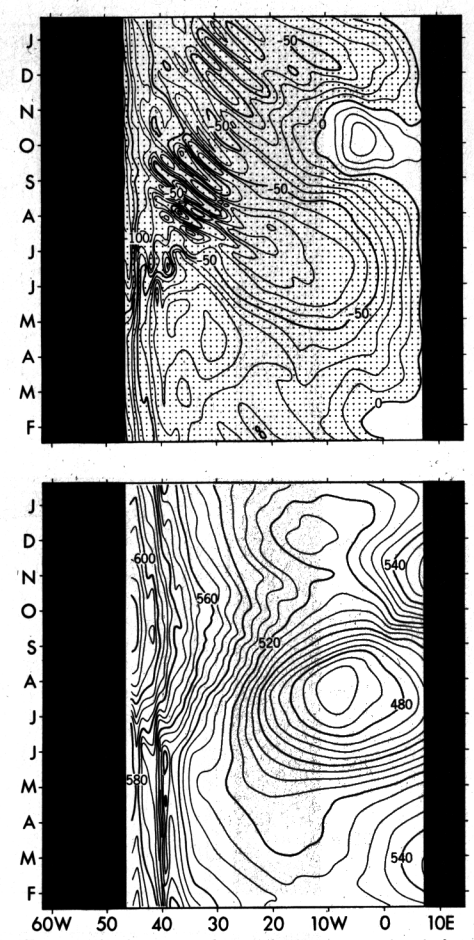

Fig. 6. Seasonal changes along the equator (top) in the zonal component of the surface current and (bottom) in the heat storage of the upper ocean. The heat storage is defined to be the integral of the temperature over the upper 317 m and has units of 10^3 cal cm^{-2}. The contour interval for the current is 10 cm s^{-1}; motion is westward in shaded regions.

Even though the seasonal changes in different parts of the tropical Atlantic are correlated with seasonal changes in the local winds, the ocean in each region cannot simply be responding to local winds. If the response were local, then it should be the same wherever the trades are intensifying. This is not so because the strengthening of the trades in May and June causes the thermocline to sink in the west but to shoal in the east. Further evidence for a nonlocal response comes from maps of the annual harmonic of the wind components and of the oceanic dynamic topography. They are strikingly different: the maps of the wind components each have a single maximum in the western Atlantic to the north of the equator; the map for the dynamic topography has two maxima, one in the west and the other in the Gulf of Guinea (Figure 4). In the west there is a high correlation between seasonal changes in the depth of the thermocline and changes in the curl of the wind. The annual harmonic in each case has a phase change of 180° across 8°N approximately (Figure 4). It appears that local Ekman suction is an important contributor to oceanic variability to the north of the equator in the west [*Garzoli and Katz*, 1983]. Figure 4 also shows that the annual harmonic of thermocline movements along the equator has a large change in phase near 20°W. This apparent nodal point for movements of the

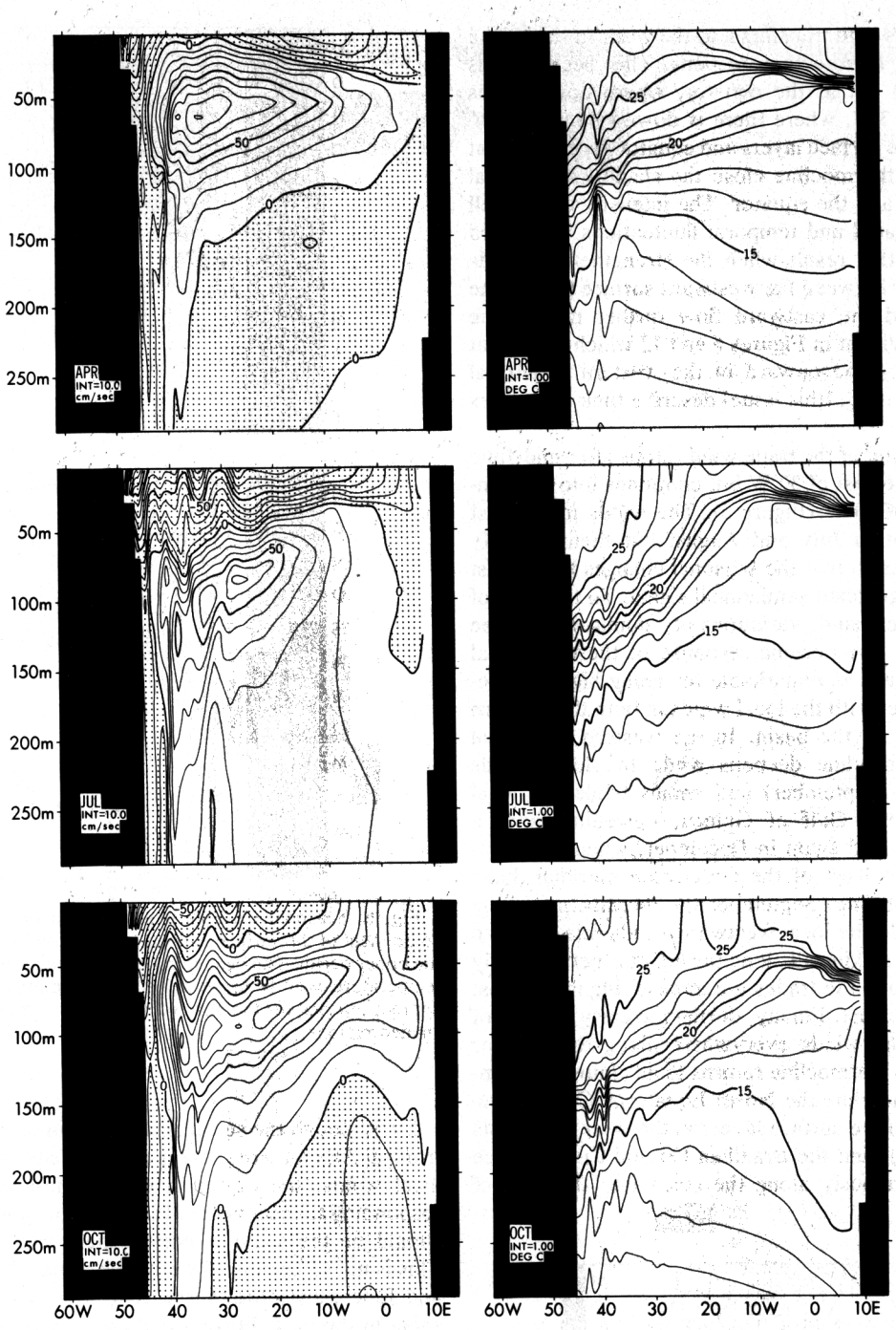

Fig. 7. Sections, along the equator, of (left) the zonal current and (right) temperature on April 15, July 15, and October 15. Motion is westward in shaded areas. The contour intervals are 10 cm s^{-1} and 1°C.

thermocline in the equatorial plane is not a feature of the seasonal cycle, however, because several harmonics contribute to the seasonal cycle. Changes in the equatorial plane are discussed in more detail in the next section.

4. Seasonal Variations in the Equatorial Zone

The winds along the equator have complicated zonal variations in their time dependence. The largest seasonal changes in the winds are near the coast of Brazil, where an annual harmonic is dominant. Wind variations to the east of 30°W have a smaller amplitude than those to the west and also have a distinct semiannual harmonic with maxima in June and July and in November (Figure 5). The oceanic response to these winds is surprisingly local (Figure 6). In the west the equatorial thermocline deepens, as long as the winds intensify, through August. This deepening is not entirely at the expense of the east because the shoaling of the equatorial thermocline east of 20°W stops at the end of June when the local westward winds start to relax. The average temperature of the entire equatorial zone therefore increases in July and August. There is not merely a zonal redistribution of warm surface waters in the equatorial zone but there are also cross-latitudinal fluxes which make it possible for thermal changes near the equator to be highly correlated, and in phase, with local changes in the wind in both the west and east. The only region where local correlations with the

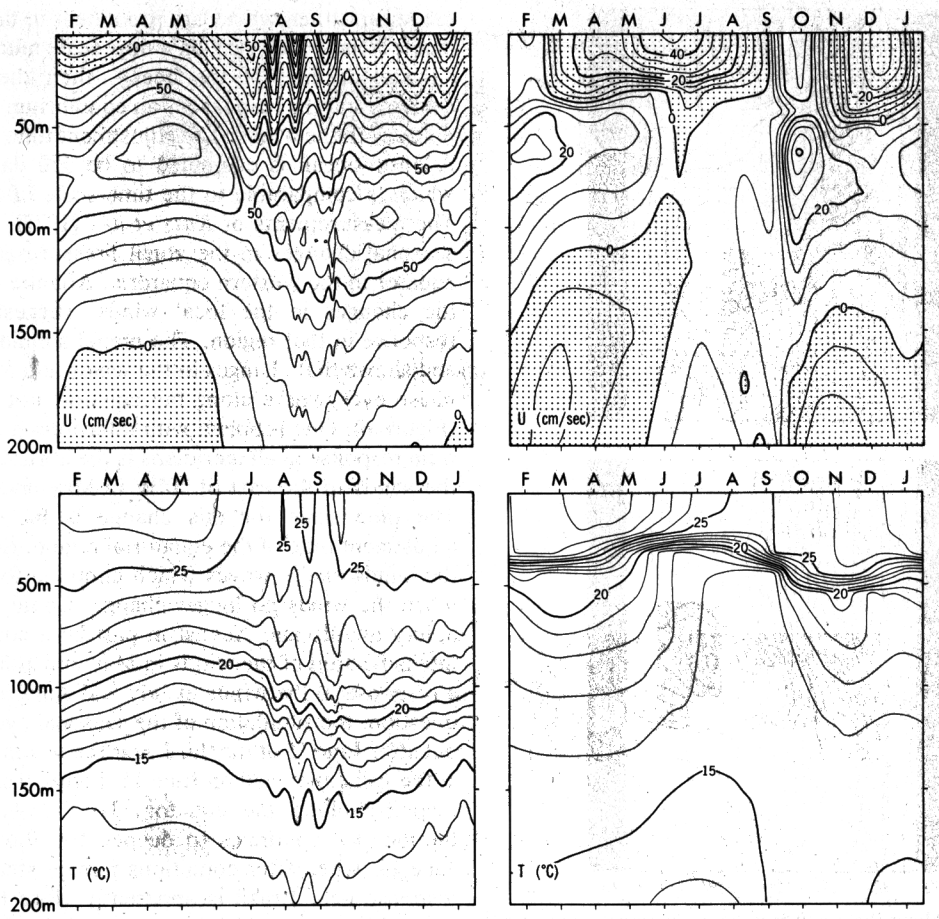

Fig. 8. Variations in (top) zonal velocity components and (bottom) temperature, as a function of depth and time, at 30°W and 0°W on the equator. Motion is westward in shaded areas.

winds are poor is to the east of the Greenwich meridian, but even here the pronounced downward slope of the thermocline to the east in the nonlinear model in October (Figure 6) is attributable to the local eastward winds at that time. The distinct semiannual signal in the eastern region implies that the Gulf of Guinea is affected primarily by the winds to the east of 30°W and secondarily by the winds near Brazil. The response of an equatorial region to remote forcing depends on both the intensity and zonal extent of the forcing [*McCreary*, 1976; *Philander*, 1981]. The winds east of 30°W are less intense than those in the west, but their larger zonal extent appears to be the deciding factor. This is confirmed by Figure 10 which shows a very high correlation between the zonal surface component on the equator at 0°W and the integral, between 35°W and 0°W along the equator of the zonal wind. There is, however, more to the semiannual signal in the east, as we shall shortly see.

To the west of 5°W there is equatorial upwelling throughout the year. It is at a maximum in the region where the westward wind is most intense (near Brazil), at a time when that wind is at a maximum (late in the boreal summer). In other words, the deepening of the equatorial thermocline in the west occurs in spite of intense equatorial upwelling. This upwelling is relatively shallow, however, and is part of a meridional cell that includes downwelling near 3°N in the west. The mass budget is discussed in detail in a companion paper [*Philander and Pacanowski*, this issue]. Here we point out that vertical movements of the thermocline need not reflect the sign of the vertical velocity component.

Figure 7 depicts the vertical structure of the thermal field and the zonal currents along the equator. When the winds are weak in April, the slope of the isotherms, the intensity of the westward surface flow, and the depth of the core of the Equatorial Undercurrent are all at a minimum. The intensification of the westward winds during the subsequent months causes the thermocline to shoal in the east, especially near 10°W, and to deepen near the coast of Brazil. In the west this change is accompanied by an increase in the depth of the layer of westward surface flow and in the depth of the core of the Equatorial Undercurrent and by a relatively small decrease in the maximum speed of the Equatorial Undercurrent (Figure 8).

Whereas an annual harmonic is dominant in the western side of the basin, a semi-annual harmonic is prominent in the east (Figure 8). The vertical structure of the motion is also more complex in the east than in the west. To the east of 10°W, for example, isotherms in the upper 50 m slope down toward the east, especially in October when the local eastward winds are most intense, but isotherms between 50 m and 150 m slope upward toward the east except in June, July, and August when there are practically no thermal gradients at depth along the equator in the east (Figure 7). In the absence of zonal gradients below 50 m the Equatorial Undercurrent fails to penetrate further east than the Green-

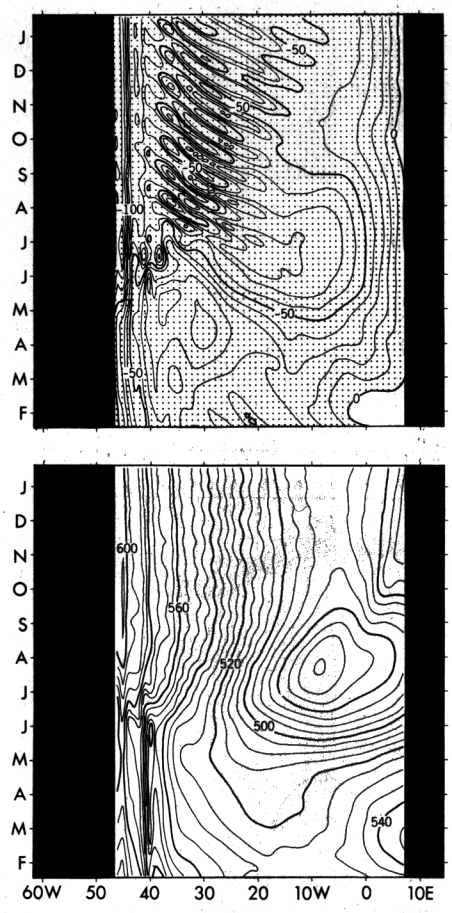

Fig. 9. Changes along the equator (top) in the zonal component of the surface current and (bottom) in the heat content of the upper 317 m of the ocean when the winds are steady after June 15. Units are cm s^{-1} (westward flow in shaded areas) and 10^3 cal cm^{-2}.

wich meridian, but from October until May the undercurrent penetrates right to the coast of Africa. Whether the dynamics of the eastward undercurrent in the Gulf of Guinea is similar to that of the undercurrent in the west is unclear. In the west the undercurrent is in the thermocline, which slopes upward to the east. In the east the undercurrent is below the thermocline and appears to be an eastward extension of the flow at the same depth in the western part of the basin. The motion below the thermocline is very different in linear and nonlinear versions of the model [*Philander and Pacanowski*, 1986]. A possible reason is the following. In a linear model, disturbances arrive below the thermocline by propagating through the fixed, specified thermocline. In a nonlinear model, vertical movements of the thermocline itself can directly force motion in the deep ocean. In the Gulf of Guinea the local eastward winds preclude an undercurrent in the thermocline, but the vertical movements of the thermocline in the west could drive eastward flow below the thermocline in the east. An equatorial Kelvin wave presumably plays a role in establishing such a current. Plots of variations at a fixed depth (50 m, for example) as a function of time and longitude do show eastward phase propagation, but other features of a Kelvin wave are difficult to identify because various other waves are superimposed.

The oceanic response to variable winds depends on the time scale of the changes in the wind. If the wind variations are abrupt, then waves are prominent in the oceanic adjustment. If the winds vary on a time scale much longer than the adjustment time of the ocean, then the waves are not evident, and the response is an equilibrium one practically in phase with the winds. The adjustment time for the equatorial Atlantic ocean is estimated to be 150 days [*Cane*, 1979], which is comparable to the time scale of the annual cycle. The measurements of *Katz et al.*, [1977], which show that seasonal changes in the zonal pressure gradient along the equator in the western equatorial Atlantic are in phase with the changes in the local winds, suggest an equilibrium response in that region. The model simulates this response and shows that changes in the winds and in the ocean are in phase everywhere along the equator, not only in the west (Figure 6). One problem with interpreting this is an equilibrium response at all meridians is the abrupt intensification of the winds to the east of 30°W in May and June (Figure 5). The time scale for this change is far shorter than the adjustment time of the equatorial region. Sudden changes in the winds excite waves which continue to be evident even when the winds no longer change. Could the oceanic variability in July and August in part be a consequence of the intensification of the winds in May and June and not merely a response to the winds in July and August? To answer this question, the simulation of the seasonal cycle was repeated, but after June 15 of the third year the winds were kept steady at the value they had on June 15. Figure 9 shows the oceanic response along the equator. To the west of 30°W the thermocline continues to deepen for about a month after June 15, whereafter conditions remain steady. The oceanic response near Brazil is apparently close to an equilibrium one. This is not so in the eastern side of the basin, where transients persist longer and even reverse trends. For example, the thermocline in the Gulf of Guinea continues to shoal into July, but then it starts to deepen, and the local westward surface current starts to decelerate, even though the winds are steady. Figure 10 shows the zonal current on the equator at the Greenwich meridian when the winds vary seasonally (solid curve) and when the winds are steady after June 15 (dashed curve). The variations in the two curves have essentially the same phase. In other words, the weakening of the actual winds in July and August contributes only partially to the oceanic changes in the Gulf of Guinea during those months. The intensification of the winds in May and June influences the oceanic response in the east for at least 2 more months and is in part responsible for the semiannual signal in the east. Equatorial Kelvin and Rossby waves must contribute significantly to this response even though the complex spatial and temporal structure of the wind makes them difficult to identify.

The relaxation of the westward winds east of 30°W during July and August amplifies the response the ocean would have had anyway, so that the deceleration of the westward surface flow, the deepening of the thermocline, and the decrease in equatorial upwelling are enhanced. In fact, the enhancement is so large that eastward surface currents and equatorial downwelling appear in the Gulf of Guinea in September and October. The eastward currents are driven not only by the relaxation of the westward tradewinds but also by the eastward winds to the east of the Greenwich meridian. To assess the importance of those eastward winds and to determine the extent to which the equatorial zone responds primarily to the winds along the equator, the

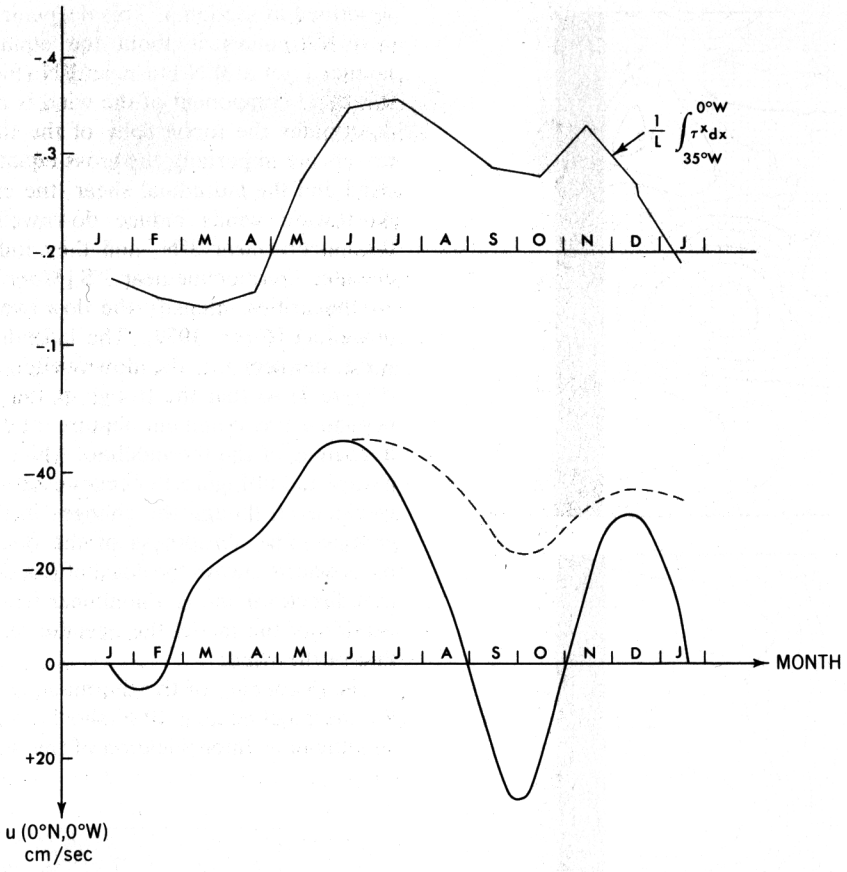

Fig. 10. The integral of (top) the zonal component of the wind stress along the equator between 35°W and 0°W and (bottom) the zonal component of the surface current on the equator at 0°W. (Positive flow is eastward). The dashed line is from the simulation in which the winds are steady after June 15.

following experiment was performed. The geometry of the ocean basin was altered by replacing the South American coast with a wall along 35°W. This modified basin was then forced with the wind stress (T^x, T^y) where

$$T^x = \tau^x(x, y = 0) \qquad \tau^x < 0$$

$$T^x = 0 \qquad \tau^x > 0$$

$$T^y = 0$$

Here x denotes longitude, y is latitude with $y = 0$ the equator, and τ^x is the zonal component of the climatological winds. The imposed winds are either westward or zero and are independent of latitude so that the curl is zero. The westward winds at the equator now prevail at all latitudes. The calculations were started by forcing the ocean with the new January winds for 1 year, by which time steady conditions obtained. The winds T were then imposed. Figure 11 shows the response along the equator. It is remarkably similar to that depicted in Figure 6. In other words, the oceanic variability along the equator to the east of 35°W is determined primarily by the westward winds over that region, and in a given year the variability is fairly independent of that during the previous year. We noted earlier that the eastward surface currents in September and October in the Gulf of Guinea are not simply a response to local eastward winds but are in part driven by zonal pressure gradients that are unbalanced when the westward winds west of the Greenwich meridian relax in July and August. One feature that is entirely attributable to the eastward winds is the downward slope of isotherms towards the African coast. Note the change in the shape of the minimum of the heat storage, which is near 10°W in Figure 6 but which is stretched longitudinally in Figure 11.

The phases of the seasonal changes in Figure 11 are so close to those in Figure 6 that as far as the Gulf of Guinea is concerned, the coast of South America is effectively at 35°W. The proximity of the northeastern Brazilian coast to the equator to the west of 35°W is one factor that effectively shrinks the equatorial Atlantic. (Rapid westward traveling coastal Kelvin waves affect the adjustment of the equatorial zone in that region.) Another factor that minimizes the effect of the winds west of 35°W on the eastern equatorial Atlantic is the gradualness of the wind variations. *Cane and Moore* [1981] have shown that low-frequency equatorial Kelvin waves plus all their reflections (long Rossby waves) at the eastern coast of an ocean basin affect only the depth of the thermocline; neither the slope of the thermocline nor the currents near the eastern coast is affected. Hence the low-frequency wind variations west of 35°W are unlikely to influence conditions other than the absolute depth of the thermocline in the Gulf of Guinea.

The upper ocean, above the thermocline, adjusts most rapidly to a change in the winds because the adjustment in that region is effected by the gravest vertical modes. Slowly propagating higher modes play an important role in the adjustment of the deeper ocean [*Philander and Pacanowski*, 1981]. The assumption that the seasonal changes in the equatorial Atlantic can be treated as an initial value problem

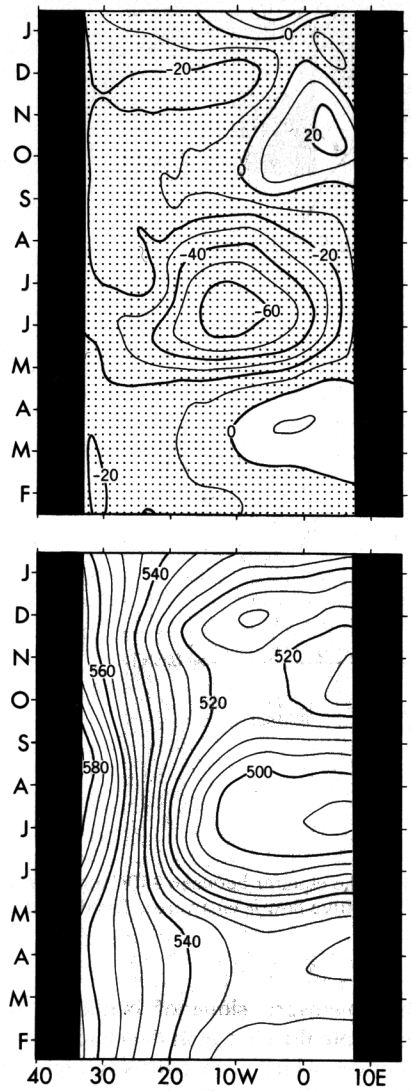

Fig. 11. As for Figure 9 but for a modified basin with a western coast along 35°W, forced with strictly westward winds which are independent of latitude and which correspond to those along the equator. (The winds in Figure 5 prevail at all latitudes but are set equal to zero in the eastern region where they are positive.)

is therefore reasonable for the upper ocean, which has a short memory, but not for the region below the thermocline, which takes much longer to come into equilibrium. Differences between the simulation of the seasonal cycle and the calculation in which the modified basin is forced with winds T should therefore be most pronounced below the thermocline. This is indeed found to be the case, especially below the thermocline in the eastern side of the basin. It follows that if the winds over the equatorial Atlantic are unusual for 1 year, then indicators of the unusual winds will persist longest below the thermocline.

This discussion of variations along the equator did not cover asymmetries about the equator. The next two sections describe such features.

5. Variability in the Western Tropical Atlantic

The intensification of the westward equatorial surface currents from April onward transfers warm surface waters westward and deepens the thermocline in the west as was described in section 4. This deepening of the thermocline is very asymmetrical about the equator and is most pronounced not at 0°N but near 3°N (Figure 3). It is clear that the zonal component of the wind is not the only factor that determines the topography of the thermocline. Two other factors are important: the cross-equatorial component of the wind and the latitudinal shear (the curl) of the zonal wind. Northward winds induce downwelling and a depressed thermocline near 3°N, and they induce upwelling and an elevated thermocline near 3°S [*Moore and Philander*, 1977]. Nonlinearities intensify the downwelling but minimize the upwelling [*Cane*, 1979]. The latitudinal shear of the zonal wind supplements the downwelling north of the equator (Figure 4) so that the trough of the thermocline along 3°N becomes the dominant feature of the thermal field. The deepening of the thermocline, which starts in April, is very abrupt and in Figure 12 occurs essentially over a period of 6 weeks even though the changes in the winds are far more gradual. The abruptness of the deepening becomes more pronounced toward the coast of Brazil (the winds intensify in that direction) and is a nonlinear feature because in a linear version of the model the oceanic response is as gradual as that of the wind.

The deepening of the thermocline near 3°N occurs while the thermocline near 10°N shoals. This is associated with a simultaneous intensification of the westward South Equato-

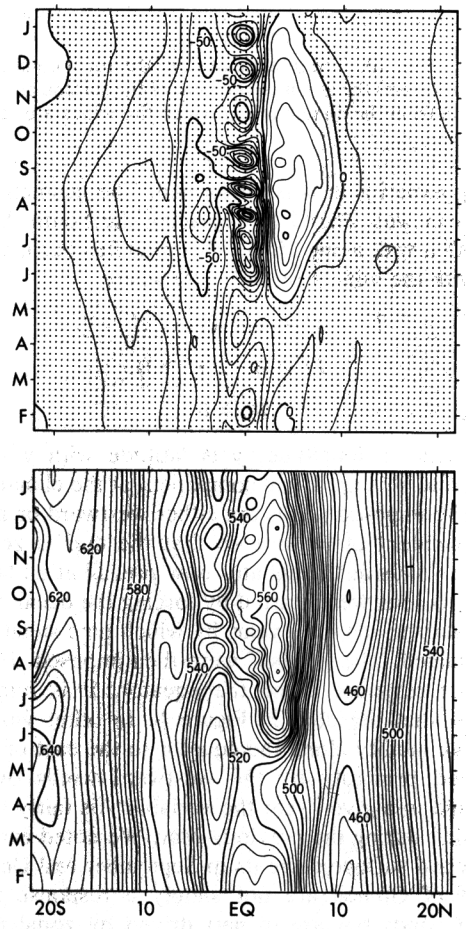

Fig. 12. Seasonal changes along 30°W (top) in the zonal component of the surface current in units of centimeters per second (flow is westward in shaded regions) and (bottom) in the heat content of the upper 317 m of the ocean in units of 10^3 cal cm^{-2}.

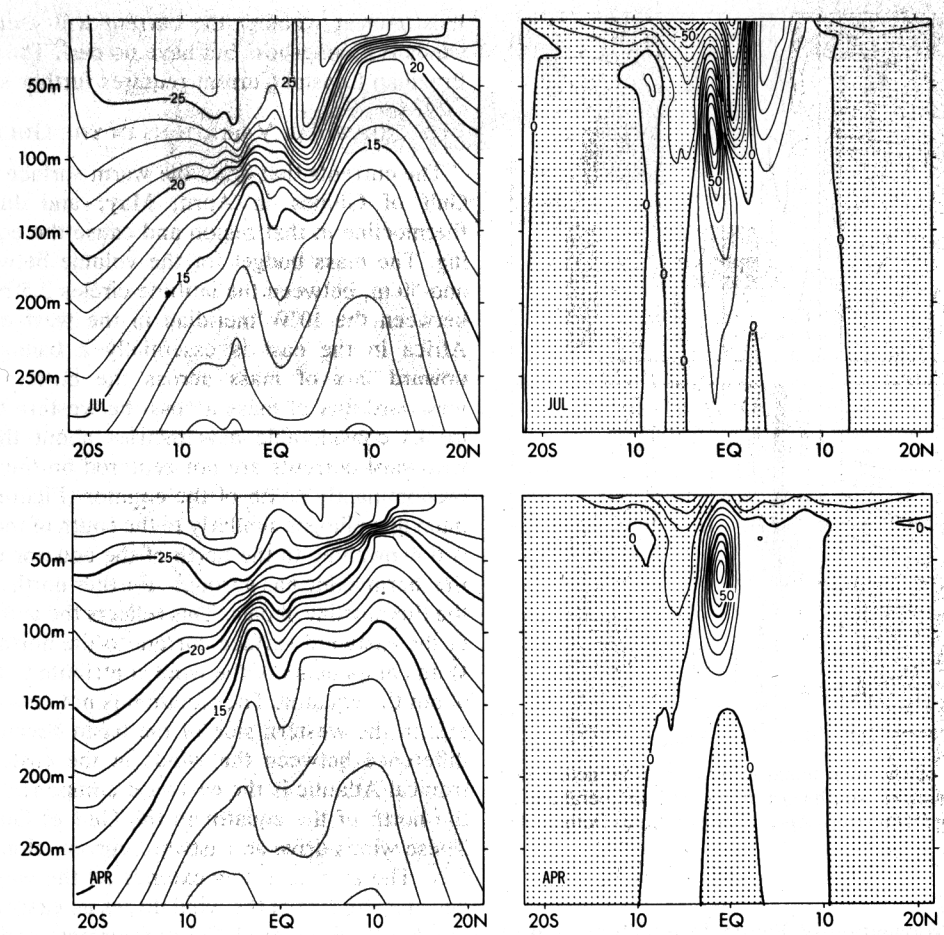

Fig. 13. Sections of the zonal current in centimeters per second (flow is westward in shaded areas) across 30°W on the right, and sections of the temperature in degrees Celsius along 30°W on the left on (top) April 15 and (bottom) July 15.

rial Current (primarily to the north of the equator) and the eastward North Equatorial Countercurrent (Figure 12). The increase in latitudinal shear results in the unstable waves mentioned earlier. The westward surface flow near the equator has a complex vertical structure in a meridional plane. In Figure 13 the South Equatorial Current is seen to be shallow at the equator but to penetrate to a considerable depth to the north of the equator during the boreal summer. The westward component of the wind, which is part of the driving force for this current, induces equatorial upwelling and thus advects eastward momentum from the Equatorial Undercurrent into the surface layers. This causes the westward surface flow to have a minimum at the equator. Another driving force for the South Equatorial Current is the northward component of the wind. In a linear model this wind drives westward Ekman drift to the south of the equator. In a nonlinear model, however, there is northward advection of westward momentum across the equator. This, together with downwelling near 3°N induced by the northward winds, cause the deep penetration of the westward current near 3°N. The northward winds also maintain a southward pressure force. This drives southward flow across the equator at the depth of the thermocline and displaces the core of the Equatorial Undercurrent southward during the summer, as is shown in Figure 13, and as explained by *Charney and Spiegel* [1971].

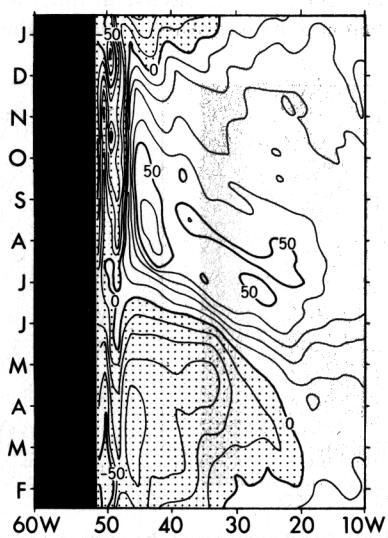

Fig. 14. Zonal velocity variations (in centimeters per second) at the surface as a function of time along 5°N. Motion is westward in shaded regions.

Though zonal phase propagation, as evidence of waves, is difficult to discern along the equator, it is a prominent feature off the equator, in the North Equatorial Countercurrent, for example (Figure 14). This suggestion that Rossby waves are involved in the adjustment of the countercurrent to the intensification of the winds is corroborated by the calculation in which the winds are held steady after June 15. The

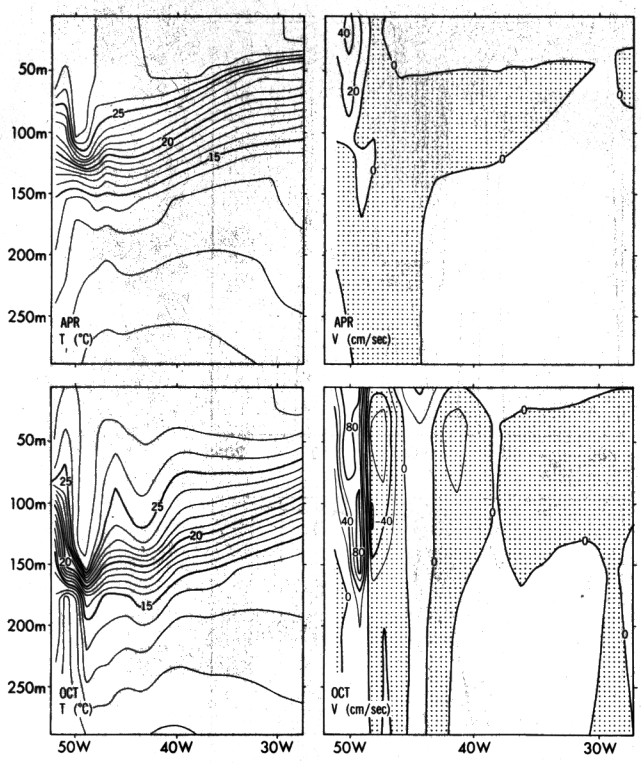

Fig. 15. Sections of the meridional current in centimeters per second (shading indicates southward flow) and temperature in degrees Celsius along 5°N on (top) April 15 and (bottom) October 15.

westward phase propagation of Figure 14 is still present in that calculation. Why the eastward countercurrent, which attains speeds in excess of 50 cm s^{-1}, does not halt the westward propagating Rossby waves which have slower speeds needs to be investigated.

The intensification of the North Equatorial Countercurrent from late May onward requires a source of mass at its origin in the west. The Brazilian Coastal Current, which veers offshore near 5°N once the winds intensify, provides the mass and continues to do so until the end of the calendar year. The current is most intense during this period and can attain speeds in excess of 130 cm s^{-1}. Between January and June, maximum speeds are smaller by a factor of 2 at least, and the current flows continuously into the Gulf of Mexico. Figure 15 shows sections across the current in April and October. The eddy that forms near 5°N when the current turns offshore (Figure 3) is evident even at a depth of 100 m. Some of this water feeds the Equatorial Undercurrent.

As in the case of the Somali Current in the Indian Ocean, both the local winds near the Brazilian coast and the curl of the wind further offshore influence the Brazilian Coastal Current. The curl of the wind, the principal driving force for the North Equatorial Countercurrent, dictates that the western boundary current veer offshore near 5°N when the countercurrent is an intense eastward surface current from late May onward. During this period a second factor comes into play: the winds change from being perpendicular to the coast to being zonal, so that they have a large component parallel to the coast (Figure 2). The alongside winds drive a coastal current and induce coastal upwelling. In the model both the coastal current and the upwelling are most intense when the winds are most intense in September and October. It is unclear whether the current will veer offshore if the winds are alongshore but have no curl. The dynamics of the Brazilian Coastal Current requires further study.

6. Seasonal Variations in the Gulf of Guinea

The currents that drain the warm surface waters from the Gulf of Guinea in April, May, and June elevate the thermocline in that region and cause the equatorial upwelling. The mass budget for the volume between the surface and 50 m, between the latitude circles 2.5°N and 2.5°S, and between the 10°W meridian in the west and the coast of Africa in the east is essentially a balance between the upward flux of mass across the bottom surface and a westward flux of mass across the western face. This result masks considerable asymmetries about the equator. The westward currents are not centered on the equator but are predominantly south of the equator (Figure 16). The maximum upwelling is similarly to the south of the equator. There is downwelling to the north of the equator near 3°N, where the thermocline has a trough. Further north toward the coast the thermocline shoals. This reflects the geostrophic balance of the eastward surface current to the north of the equator. Both components of the wind contribute to the asymmetries about the equator. The situation is not entirely analogous to that in the western side of the basin because an important difference between the winds in the eastern and western tropical Atlantic is the eastward component of the winds to the north of the equator in the Gulf of Guinea (Figure 2). These winds drive an eastward current along the coast near 5°N. The eastward flow extends all the way to the equator because the curl of the wind drives an eastward extension of the North Equatorial Countercurrent, and the northward component of the wind drives eastward Ekman drift which is very intense near 3°N where the thermocline is depressed [*Moore and Philander*, 1977]. The westward flow to the south of the equator is driven by the westward winds near the equator and by the northward winds which elevate the thermocline near 3°S.

The seasonal changes in the zonal surface currents are highly correlated with the seasonal changes in the winds to the east of 30°W (Figures 10 and 16). The westward surface current, for example, is most intense in June, when both the northward wind and the westward wind near the equator are

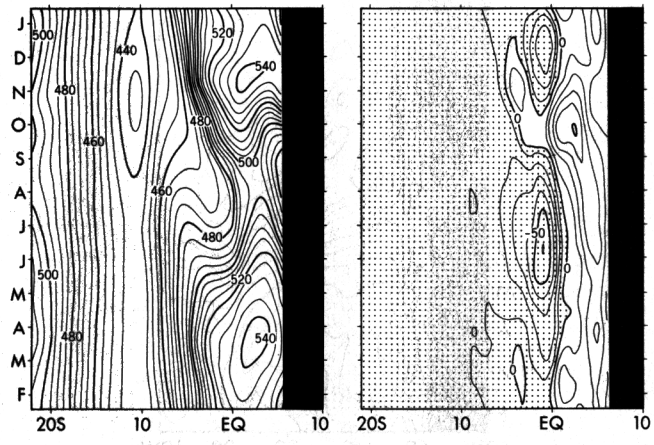

Fig. 16. (right) Zonal currents at the surface and (left) the heat storage of the upper 317 m along 0°W as a function of time. Units are centimeters per second and 10^3 cal cm^{-2} respectively. Motion is westward in shaded areas.

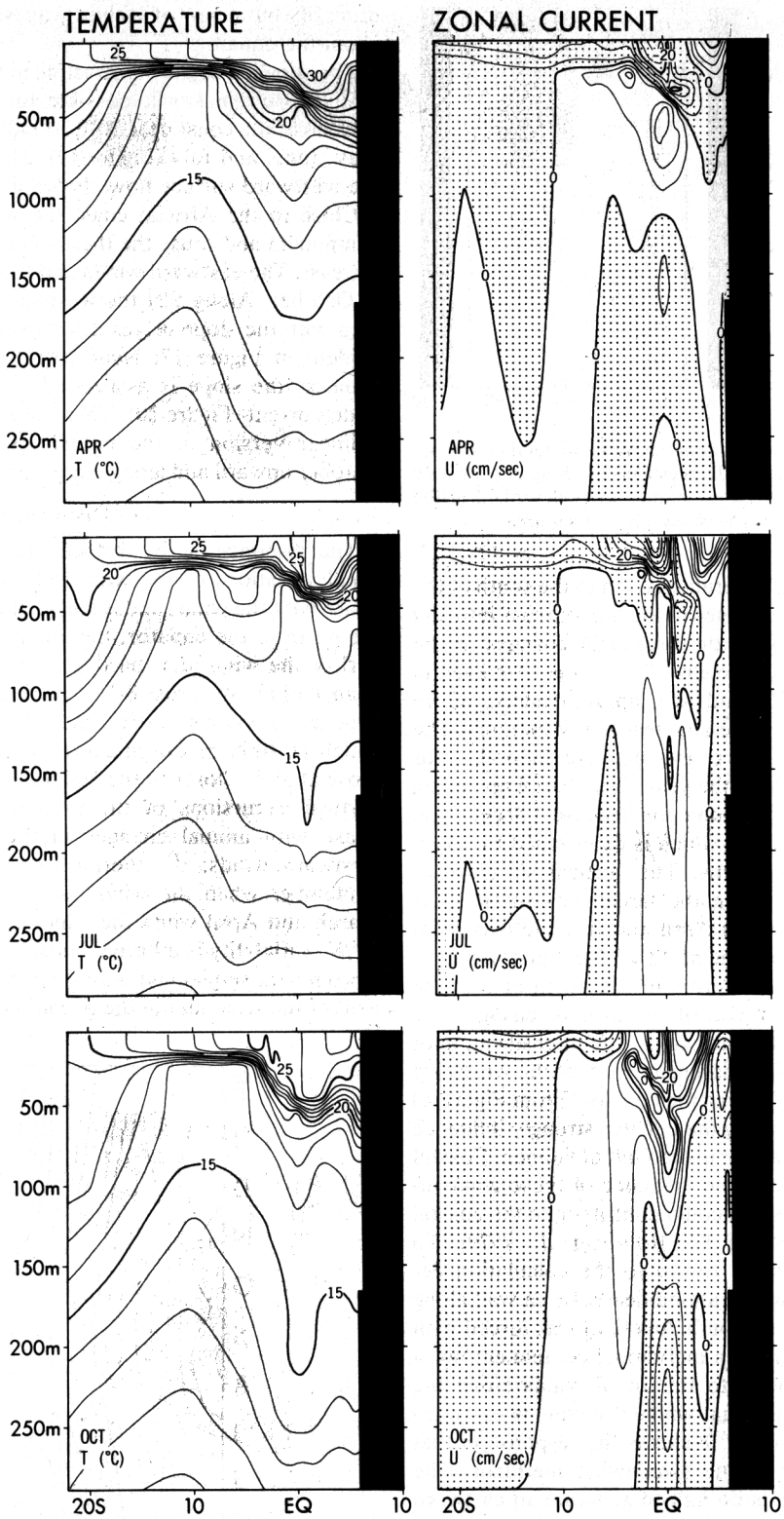

Fig. 17. Sections of (right) the zonal currents and (left) temperature along 0°W on April 15, July 15, and October 15. Motion is westward in shaded areas.

most intense. This westward current practically disappears in October, when the eastward winds have their largest zonal extent (Figure 5). The reappearance of westward flow in November and December coincides with the reintensification of the westward equatorial winds during those months, primarily to the east of 30°W (Figures 5 and 10).

The westward surface flow out of the Gulf of Guinea from April onward causes an elevation of the thermocline in the eastern tropical Atlantic, as was pointed out in section 4. From July onward the thermocline in the east starts to deepen again as the local westward winds begin to relax. The depth reaches a maximum in October when there is eastward

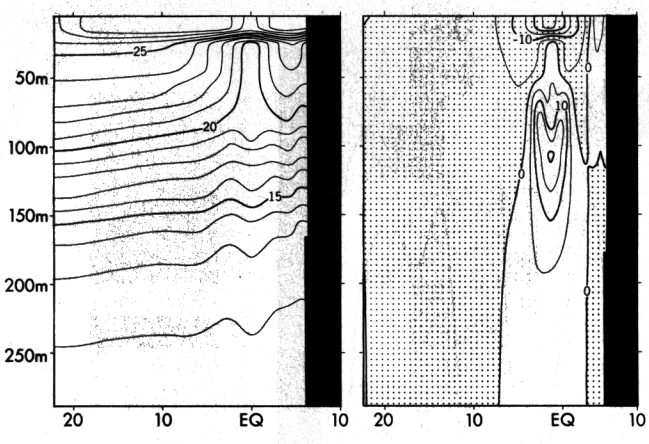

Fig. 18. Sections of (right) the zonal currents in centimeters per second and (left) temperature in degrees Celsius along 0°W on July 15 when the winds and basin are modified as is described in the caption of Figure 11. Motion is westward in shaded areas.

flow across the Greenwich meridian, even to the south of the equator. These seasonal changes in the flux of mass into and out of the Gulf of Guinea cause seasonal changes in the large-scale thermal field of the east. This is the case even in coastal regions, along 5°N and 10°E approximately, where the local winds may not have any seasonal variations. The winds are parallel to these coasts and are favorable for coastal upwelling throughout the year. The coastal upwelling is nonetheless a seasonal phenomenon because it depends on the depth of the thermocline, which is determined by large-scale, not by local, conditions. The vertical structure of these seasonal changes along the Greenwich meridian is shown in Figure 17. Between April and July the maximum speed of the eastward current north of the equator practically doubles while the isotherms to the north of 3°N are elevated. Several factors contribute to this change: the intensification of the northward winds, the intensification of the curl of the wind, and the intensification of the westward winds (to the west of 0°W) along the equator. From Figure 10 it is clear that the winds along the equator strongly influence the surface flow at the equator in the Gulf of Guinea. Coastal Kelvin waves could extend the influence of these winds to the African coastal zones and could contribute to the coastal upwelling in Figures 16 and 17 [*Moore et al.*, 1979]. To evaluate this hypothesis we return to the calculation described in section 5, in which a modified basin (a wall along 35°W replaced the coast of South America) was forced with winds T, which have neither a meridional component nor a curl and which correspond to the zonal winds along the equator in Figure 5, except that where the wind is eastward it is set equal to zero. Figure 18 shows the response of that model, on July 15, along the Greenwich meridian. The westward equatorial winds do indeed generate an eastward coastal current and elevate the isotherms near the coast, but the amplitude of these features is very small in comparison with that of the features in Figure 17. This implies that the westward winds along the equator have a secondary effect on the coastal upwelling near 5°N. The curl of the wind to the north of the equator and the northward component of the wind are more important in determining seasonal changes at the coast. The asymmetry about the equator of the zonal flow in Figure 16 corroborates this conclusion because the winds along the equator in the west affect the eastern region primarily by means of Kelvin waves which are symmetrical about the equator.

The shoaling of the thermocline in the Gulf of Guinea from May onward makes it possible for the northwards winds parallel to the coast near 10°E to induce coastal upwelling in May, June, and July (Figure 19). This shoaling is caused by the westward surface flow shown in Figure 17.

Close to the African coast the winds have an eastward component and cause the thermocline to slope downward to the east. The eastward winds and this slope are most intense in October. Along 5°N the westward pressure force associated with the slope drives a westward coastal undercurrent evident in Figure 17. Near 10°E and to the south of the equator, the slope is associated with a southward coastal undercurrent (Figure 20). This feature, which is absent from a linear version of the model, disperses westward from October onward and along 5°S is discernable as late as April.

7. Discussion

The response of the tropical Atlantic Ocean to the seasonal variations of the wind is to a first approximation in phase with the winds and is surprisingly local. In the west, to the north of the equator, the annual harmonics of both the curl of the wind and the dynamic topography have a 180° change of phase across 8°N approximately. Ekman pumping appears to control vertical movements of the thermocline, which at 10°N has oscillations that are out of phase with those at 3°N. Closer to the equator and to the west of 30°W, vertical excursions of the thermocline are practically in phase with annual changes in the intensity of the local westward winds: the thermocline is deep in August and September when the winds are intense and is shallow in March and April when the winds are weak. To the east of 30°W, variability is different because the equatorial zone has a prominent semiannual harmonic both in the zonal component of the wind and in the oceanic response. This response

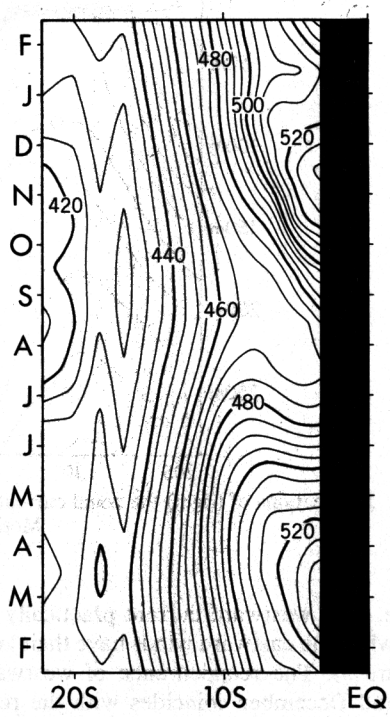

Fig. 19. Seasonal variations in the heat storage to a depth of 317 m along 10°E near the African coast. Units are 10^3 cal cm^{-2}.

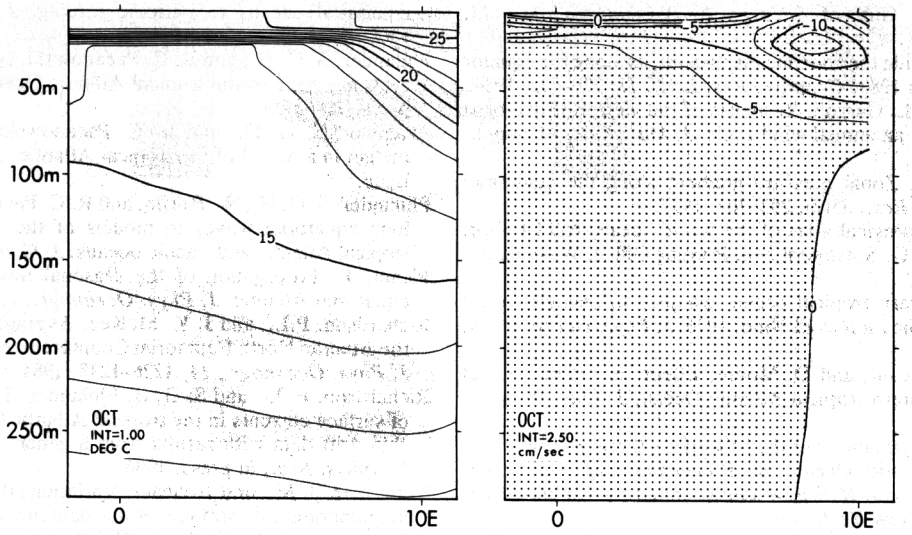

Fig. 20. (right) The meridional current across 5°S in centimeters per second (flow is southward in shaded areas) and (left) the temperature along 5°S in degrees Celsius (1°C) on October 15.

is practically in phase with the local wind: westward surface flow is most intense when the westward winds have maxima, in June and again in November. The region most affected by nonlocal winds is to the east of the Greenwich meridian but even here the local eastward winds succeed in causing isotherms to slope downward to the east in the surface layers. The slope is pronounced in October, when the eastward winds have a large zonal extent.

A response that is in phase with the forcing suggests that the ocean is in equilibrium with the winds. This is approximately the case in the western equatorial region because conditions in the west change relatively little when the winds are suddenly frozen and kept constant. This is not the case in the eastern side of the basin, however. There the prominent semiannual oscillation is in part attributable to the oceanic adjustment to the rapid intensification of the westward winds in May and June. These winds drive accelerating westward equatorial currents, but when the winds are frozen at their value on June 15, the currents decelerate and subsequently accelerate again to give an apparent semiannual oscillation (Figure 10). The transients excited by the intensification of the winds in May and June decay by December, so that the response of the surface layer of the equatorial zone to the intensification of the winds can be treated as an initial value problem. It is remarkable that the wind variations are in phase and augment variations that the ocean would have undergone anyway once the winds intensified in May and June. The possibility that there are strong interactions between the ocean and atmosphere during the seasonal cycle cannot be ruled out.

The results presented here are from a model forced with climatological winds. For the years 1982, 1983, and 1984, accurate surface winds and simultaneous oceanographic measurements with a high density in space and time, will be available because of the Seasonal Response of the Equatorial Atlantic (SEQUAL) program and the Programme Francais Océan-Climat en Atlantique Equatoriale (FOCAL) that studied the seasonal cycle of the tropical Atlantic. (The August 1984 issue of *Geophysical Research Letters* [*Weisberg*, 1984] was devoted to articles that describe preliminary results from these programs.) Simulation of variability during 1982, 1983, and 1984 will provide a stringent test for the model and will suggest improvements to the model.

Acknowledgments. During the course of this work we had the benefit of discussions with R. H. Weisberg, who suggested that transients excited by the abrupt intensification of the southeast trades in May contribute to the semiannual cycle in the Gulf of Guinea. J. Sarmiento and M. Cox made valuable comments on an earlier version of this manuscript. J. Pege and P. Tunison and his staff provided expert technical assistance.

REFERENCES

Bruce, J. G., J. Kerling, and W. Beatty, On the North Brazilian eddyfield, *Prog. Oceanogr.*, in press, 1984.

Bryan, K., A numerical method for the study of the world ocean, *J. Comput. Phys.*, *4*, 347–376, 1969.

Busalacchi, A. J., and J. Picaut, Seasonal variability from a model of the tropical Atlantic Ocean, *J. Phys. Oceanogr.*, *13*, 1564–1588, 1983.

Cane, M. A., The response of an equatorial ocean to simple wind-stress patterns, I, Model formulation and analytic results, *J. Mar. Res.*, *37*, 233–252, 1979.

Cane, M. A., and D. W. Moore, A note on low-frequency equatorial basin modes, *J. Phys. Oceanogr.*, *11*, 1578–1585, 1981.

Cane M. A., and E. S. Sarachik, The response of a linear baroclinic equatorial ocean to periodic forcing, *J. Mar. Res.*, *39*, 651–693, 1981.

Charney, J. G., and S. L. Spiegel, Structure of wind-driven equatorial currents in homogeneous oceans, *J. Phys. Oceanogr.*, *1*, 149–160, 1971.

du Penhoat, Y., and A. M. Triguier, The linear seasonal response of the tropical Atlantic Ocean, *J. Phys. Oceanogr.*, *15*, 316–329, 1985.

Garzoli, S. L., and E. J. Katz, The forced annual reversal of the Atlantic North Equatorial Countercurrent, *J. Phys. Oceanogr.*, *13*, 2082–2090, 1983.

Garzoli, S. L., and S. G. H. Philander, Validation of an equatorial Atlantic model using inverted echo sounder data, *J. Geophys. Res.*, *90*, 9199–9201, 1985.

Hellerman, S., and M. Rosenstein, Normal monthly windstress over the world ocean with error estimates, *J. Phys. Oceanogr.*, *13*, 1093–1104, 1983.

Hisard, P., Variations saisonnières à l'équateur dans le Golfe de Guinée, *Cah. ORSTOM, Ser Oceanogr.*, *11*, 349–358, 1973.

Hisard, P., and A. Morlière, La terminaison du Contre-Courant Equatorial Subsuperficiel Atlantique dans le Golfe de Guinée, *Cah. ORSTOM, Ser Oceanogr.*, *11*, 455–465, 1973.

Houghton, R. W., Seasonal variations of the subsurface thermal

structure in the Gulf of Guinea, *J. Phys. Oceanogr.*, *13*, 2070–2081, 1983.

Katz, E. J., Basin wide thermocline displacements along the equator off the Atlantic in 1983. *Geophys. Res. Lett.*, *11*, 729–732, 1984.

Katz, E. J., and S. L. Garzoli, Response of the western Equatorial Atlantic Ocean to an annual wind cycle, *J. Mar. Res.*, *40*, suppl., 307–327, 1982.

Katz, E. J., et al., Zonal pressure gradient along the equatorial Atlantic, *J. Mar. Res.*, *35*(2), 293–307, 1977.

Levitus, S., Climatological atlas of the world ocean, *NOAA Prof. Pap. 13*, 173 pp., U. S. Government Printing Office, Washington, D. C., 1982.

McCreary, J., Eastern tropical ocean response to changing wind systems with application to El Niño, 1976, *J. Phys. Oceanogr.*, *6*, 632–645, 1976.

McCreary, J., J. Picaut, and D. Moore, Effects of remote annual forcing in the eastern tropical Atlantic Ocean, *J. Mar. Res.*, *42*, 45–81, 1984.

Merle, J., Seasonal variability of the subsurface thermal structure in the tropical Atlantic Ocean, in *Proceedings of 14th Liege Colloquium on Ocean Hydrodynamics*, edited by J. Nihoul, pp. 31–49, Elsevier, New York, 1983.

Merle, J., and S. Arnault, Seasonal variability of the surface dynamic topography in the tropical Atlantic Ocean, *J. Mar. Res.*, *43*, 267–288, 1985.

Moore, D. W., and S. G. H. Philander, Modeling of the tropical oceanic circulation, in *The Sea*, vol. 6, pp. 319–361, Interscience, New York, 1977.

Moore, D. W., P. Hisard, J. P. McCreary, J. Merle, J. J. O'Brien, J. Picaut, J. M. Verstraete, and C. Wunsch, Equatorial adjustment in the eastern Atlantic, *Geophys. Res. Lett.*, *5*, 637–640, 1978.

Pacanowski, R., and S. G. H. Philander, Parameterization of vertical mixing in numerical models of tropical oceans, *J. Phys. Oceanogr.*, *11*, 1443–1451, 1981.

Philander, S. G. H., The response of equatorial oceans to a relaxation of the trade winds, *J. Phys. Oceanogr.*, *11*, 176–189, 1981.

Philander, S. G. H., and R. C. Pacanowski, The generation of equatorial currents, *J. Geophys. Res.*, *85*, 1123–1136, 1980.

Philander, S. G. H., and R. C. Pacanowski, The response of equatorial oceans to periodic forcing, *J. Geophys. Res.*, *86*, 1903–1916, 1981.

Philander, S. G. H., and R. C. Pacanowski, Nonlinear effects in the seasonal cycle of the tropical Atlantic Ocean, *Deep Sea Res.*, in press, 1986*a*.

Philander, S. G. H., and R. C. Pacanowski, The mass and heat budget in a model of the tropical Atlantic, *J. Geophys. Res.*, this issue.

Philander, S. G. H., W. Hurlin, and R. C. Pacanowski, Properties of long equatorial waves in models of the seasonal cycle in the tropical Atlantic and Pacific oceans, *J. Geophys. Res.*, this issue.

Picaut, J., Propagation of the seasonal upwelling in the eastern equatorial Atlantic, *J. Phys. Oceanogr.*, *13*, 18–37, 1983.

Richardson, P.L., and J. K. McKee, Average seasonal variation of the Atlantic North Equatorial Countercurrent from ship drift data, *J. Phys. Oceanogr.*, *14*, 1226–1238, 1984.

Richardson, P. L., and S. G. H. Philander, The seasonal variations of surface currents in the tropical Atlantic Ocean: Comparison of ship drift data with results from a general circulation model, *J. Geophys. Res.*, in press, 1986.

Verstraete, J. M., and J. Picaut, Variations du niveau de la mer, de la température de surface, et des hauteurs dynamiques le long de la côte nord du Golfe de Guinée, *Oceanogr. Tropicale*, *18*, 139–162, 1983.

Voituriez, B., Les variations saisonneirès des courants equatoriaux à 4°W et l'upwelling equatorial du Golfe de Guinée, *Oceanogr. Trop.*, *18*, 169–199, 1983.

Weisberg, R. H., SEQUAL/FOCAL: First year results on the circulation in the equatorial Atlantic, *Geophys. Res. Lett.*, *11*, 713–714, 1984.

Weisberg, R. H., and T. Y. Tang, Equatorial ocean response to growing and moving wind systems with application to the Atlantic, *J. Mar. Res.*, *41*, 461–486, 1983.

R. C. Pacanowski and S. G. H. Philander, Geophysical Fluid Dynamics Laboratory, NOAA, Princeton University, P.O. Box 308, Princeton, NJ 08542.

(Received January 21, 1986;
accepted March 7, 1986.)